Dumbbell shaped inline Mach–Zehnder interferometer for sensor applications

A. LOKMAN, N. IRAWATI[a], H. AROF[*], S. W. HARUN[a], N. M. ALI
Department of Electrical Engineering, Faculty of Engineering, University of Malaya, 50603, Kuala Lumpur, Malaysia
[a]Photonics Research Center, University of Malaya, 50603, Kuala Lumpur, Malaysia

A compact dumbbell-shaped inline Mach-Zehnder interferometer (MZI) is proposed for sensing temperature, refractive index and relative humidity (RH). The MZI sensor consists of two bulges separated by a tapered waist and was fabricated using an arcing process by a fusion splicer. The fabricated MZI shows a good reflected interference spectrum where the free spectral range depends on the length of the tapered waist connecting the two dumbbells. At the tapered waist length of 0.5 cm, the reflected spectrum is observed to be responding to the change in the temperature of the surrounding medium with a sensitivity coefficient of 0.049 nm/°C. It is also found that when the refractive index of the surrounding medium increases from 1.00 to 1.36 the reflected interference spectrum of the sensor is blue-shifted linearly. Finally, the MZI sensor is coated with hydroxyethylcellulose/ polyvinylidenefluoride (HEC/PVDF) composite and the effect of changes in relative humidity to its interference spectrum is examined. It is observed that as the RH of the ambience increases, the interference wavelength of the sensor linearly shifts to longer wavelength with a sensitivity of 0.159 nm/RH%.

(Received May 12, 2014; accepted May 15, 2014)

Keywords: Microfiber, Flame Brushing Technique, Inline Mach-Zehnder Interferometer, Fiber Sensor, Hydroxyethylcellulose/ Polyvinylidenefluoride (HEC/PVDF)

1. Introduction

The use of optical fiber sensors is expanding and has now permeated into biological, chemical and environmental industries. Many fiber based sensors have been developed including those used in the measurements of the humidity, refractive index (RI), temperature, and strain [1-3]. Compared to conventional sensors based on mechanical and electrical properties, the optical fiber sensors offer many advantages since they are compact, highly sensitive, immune to electromagnetic interference, resistant to corrosion and placid to volatile surrounding. One of the most popular probes based on optical fiber is Mach–Zehnder interferometer (MZI) and it has been widely used for various sensing purposes [4-7]. For instance, inline fiber MZI sensors have been utilized for monitoring changes in refractive index, strain and temperature [1-3]. In the last ten years, many designs have been proposed for constructing MZI sensors using tapered fibers [8-10], long- period gratings (LPGs) [11, 12], two different single-mode fibers (SMFs) [13], [14] and some other special configurations [15-17].

For sensing refractive index (RI), a fraction of the fundamental core mode power leaks out as cladding modes that are sensitive to the RI of the surrounding medium. Therefore, based on this operating principle, an MZI sensor of any configuration can be employed to detect the refractive indices of liquids. Meanwhile, the difference in path lengths between the core and cladding modes (in some of the structures such as LPGs, core-offset or other insertions) usually changes with the ambient temperature and strain. It will introduce the additional optical path difference (OPD) that makes the spectra red shift or blue shift. Therefore, a temperature and strain sensitive sensor can be realized.

In this paper, a simpler inline MZI with a dumbbell-shape structure is proposed. The MZI is then used as a sensor to measure temperature, refractive index and humidity. The proposed MZI structure comprises two bulges connected by a tapered waist.

2. Fabrication and characteristic of inline MMZI

The first step in fabricating the MZI structure is to cleave an SMF into two sections, each with a flat and smooth end-surface, as illustrated in Fig. 1 (a). Then the end facets of the two sections are matched and fused using the manual "arc" function of Sumitomo Type 36 splicer. While fusing the two sections of the fiber, the "arc" function is used five times so that extra pressure is exerted from both sides to form the first bulge at the joint as shown in Fig. 1(b). Once the first bulge is formed, the jointed fiber is then cleaved once again at 5mm to 7mm away from the center of the first bulge as depicted in Fig. 1(c). Then the second bulge is formed in a similar fashion as shown in Fig. 1 (d). It should be noted that the fusion splicer softens the ends of the two fibers with heat before pulling them together to join them at the center. When the "arc" function is used repeatedly, more material is lumped at the center, thus forming a bulge, while the neck of the bulge gets thinner. When the second bulge is made, it is a bit smaller in size than the first one as less material is available from the waist area between the bulges since it

has been used in forming the first bulge. The waist area also becomes thinner because it gets tapered even more. The completed dumbbell structure is shown in Fig. 2 where the diameters of the first and second bulges are 224 µm and 218 µm respectively. The diameter of the waist section is about 81.5 µm and its length is approximately 5000 µm while the length of the whole structure is around 6780 µm. The parameters of the fusion splicer program used to fabricate the dumbbell structure are given in Table 1.

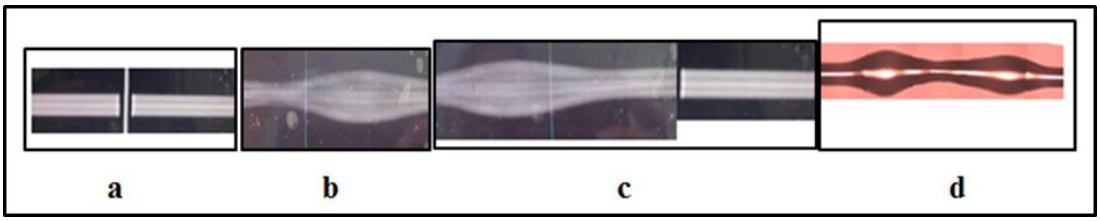

Fig. 1. Illustration of the fabrication procedure of MZI sensor.

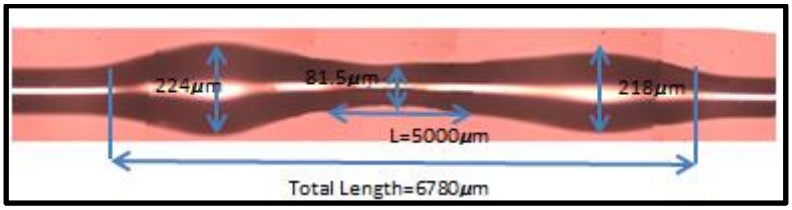

Fig. 2. The experimental view of the proposed dumbbell shape MZI.

Table 1. Parameters for fabricating the bulges.

Parameters	Units	Values
Arc duration	s	1.50
Prefusion	s	0.01
Arc Gap	µm	10.0
Overlap	µm	45.0

Fig. 3 shows the experimental setup of the proposed sensor used to measure changes in temperature, refractive index and humidity. The input and output ports of the sensor are connected to amplified spontaneous emission (ASE) laser source and optical spectrum analyzer (OSA), respectively. Dumbbells with two different tapered waist length of L=0.5cm and L=0.7cm (refer to Fig. 2) are tested to compare the relative sensitivity of the sensors. When the input light beam reaches the first bulge, it is divided into two parts where the first part continues to propagate in the core, while the other part travels in the cladding of the SMF. Due to the optical path difference (OPD) between cladding mode and core mode, an interference pattern is established when the two output beams recombine at the output end of the second bulge. The output intensity of the MZI is governed by

$$I = I_1 + I_2 + 2\sqrt{I_1 I_2}\, cos(\varphi) \quad (1)$$

where I is the intensity of the interference signal, I_1 and I_2 are the intensity of the light propagating in the fiber core and cladding respectively and φ is the phase difference between the core and cladding modes. It is approximately equal to:

$$\varphi = \left(\frac{2\pi(\Delta n_{eff})L}{\lambda}\right) \quad (2)$$

where Δn_{eff} is defined as $(n_c{}^{eff} - n_{cl}{}^{eff})$ which is the difference of the effective refractive indices of the core and the cladding modes, L is the length of the interferometer region and λ is the input wavelength. The free spectral range (FSR) of the spectrum can be expressed as:

$$FSR = \lambda^2/(\Delta n_{eff})L \quad (3)$$

Fig. 4 displays the output spectrum for the two dumbbell sensors with different length L, where the unsmooth curve is attributed to the non-uniqueness of cladding modes. It can be observed from this figure that, with the increase of the tapered waist length from 0.5 cm to 0.7 cm, the FSR around 1552 nm is decreased from 1552.66 nm to 1552.34 nm, which conforms to Eq. (3). It is also found that the insertion loss of the device goes up with the increase of the waist length. The reason is that the part of light that propagates along the air cavity will have to travel a longer distance as the waist length increases. Since the light propagating along the air cavity has a higher possibility to leak out as loss, the amount of the loss is proportional to the propagation distance.

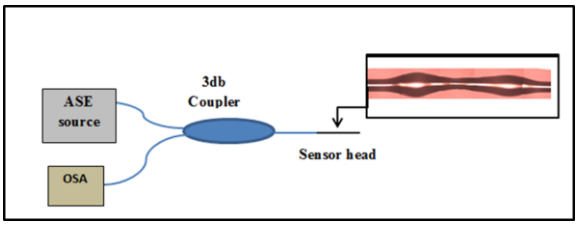

Fig. 3. The experimental setup for the proposed sensor to measure changes in temperature, refractive index and humidity.

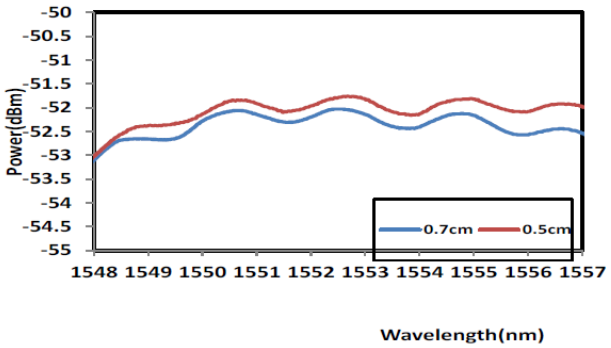

Fig. 4. The typical output spectrum of the sensor with L=0.5cm and L=0.7cm.

The temperature characterization of the dumbbell sensors with L=0.5 cm and L=0.7 cm was conducted by placing them on a hot plate where the temperature was varied from 50 to 130 Celsius. Fig. 5 shows the sensitivity coefficients for both L. It found that the sensitivity coefficients of the sensor with L=0.5cm and L=0.7cm are 0.049 nm/°C and 0.005 nm/°C, respectively. It observed that sensor with shorter L shows higher sensitivity compared to the one with longer L. Inset of Fig. 5 shows the output spectrum shift of dumbbell MZI with L=0.5cm. As seen, the output spectrum shifts to longer wavelength with the increment of the temperature. This is attributed to thermo-optic and thermal expansion effects in the interferometer, which causes changes in the effective refractive index difference between the core and the cladding modes, and the effective length of the interferometer, respectively. Both effects change the phase difference between the core and cladding modes of the propagating light and thus the interference fringes as shown in Fig. 5.

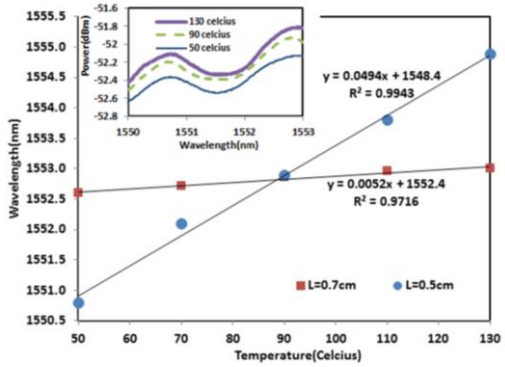

Fig. 5. Peak wavelength of the output spectrum against the temperature increment. Inset shows the output spectra at three different temperatures.

Next, we investigated the effect of the surrounding medium on the reflected spectrum from dumbbell MZI. In our experiment, the dumbbell shaped MZI probe in Fig. 3 is immersed into three different liquids namely water, alcohol and hydroxyethylcellulose / polyvinylidenefluoride (HEC/PVDF) composite, which has a refractive index of 1.33, 1.36 and 1.48, respectively. Due to the compact structure of the sensor, a single drop of the liquid solution was enough to surround the whole dumbbell shape. The MZI was cleansed with deionized water and compressed air after each measurement. The reflected spectrum is also measured with air as the surrounding medium for comparison purpose. Fig. 6 shows the reflected interference spectrum with the different surrounding materials. It could be seen that the wavelength is blue-shifted with the increase of the surrounding refractive index from 1.00 to 1.36. This is due to the phase difference between the core and cladding modes, which reduces with the increase of surrounding refractive index as described in Eq. (2). However, as the refractive index of the surrounding increases beyond the refractive index of the silica core, the peak wavelength shifts back to the longer wavelength as shown in Fig. 6. The unsmooth curve shows the variation of the surface roughness of the tapered waist. This preliminary result shows that the proposed dumbbell shaped MZI probe can be used as a refractive index sensor.

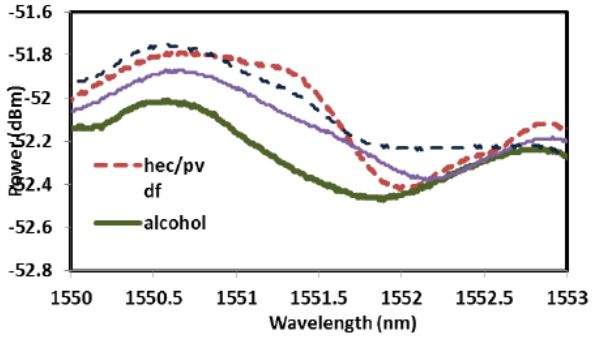

Fig. 6. The reflected interference spectra when the dumbbell MZI is embedded into various surrounding materials.

Lastly, we applied the dumbbell MZI as a relative humidity (RH) sensor. First of all, the dumbbell shaped MZI probe was coated with a polymer blend of HEC/PVDF composite, whose optical properties can change in response to the change in relative humidity of its surrounding. The configuration of the RH sensor is similar to the one shown in Fig. 3, where the input ports of the 2×13 dB coupler are connected to the ASE laser source and OSA while the output port is connected to the sensor probe. The sensor probe is placed in a sealed chamber with a dish filled with saturated salt solution. Exposing the HEC/PVDF composite to the RH changes inside the chamber has produced variations in the reflected spectrum of the MZI. In the experiment, the performance of the proposed sensor was investigated for various relative humidity ranging from 50 to 75 % using data logging humidity-temperature meter.

Fig. 7 shows the wavelengths shifting with the different level of humidity. It could be seen that the interference pattern red-shifts with the increase of the humidity percentage from 55 to 75%. This is attributed to the decrease in the refractive index of the surrounding material with the humidity. The decrease of average cladding refractive index increases the phase difference between core and cladding modes, which changes the FSR

and results in the shifting of the reflected spectrum of the MZI to the longer wavelength. The behavior of the proposed sensor against RH is investigated with and without the HEC/PVDF composite coating. The relationship between the refractive indices and wavelengths is approximately linear in the humidity ranges of 50% to 75% for both cases. Without the HEC/PVDF layer, an interference wavelength shifts from 1550.587 nm to 1550.918 nm with a linearity of more than 95% as the RH varies from 50% to 75%. The sensitivity of the sensor significantly increases when the dumbbell MZI is coated by the HEC/PVDF composite from 0.013 nm/RH% to 0.159 nm/RH%. As also shown in Fig. 8, the linear trend line can be fitted to the experimental data with a correlation coefficient value of r >0.99. These results show that the proposed sensor is applicable for relative humidity sensing and also has the ability to provide real time measurement.

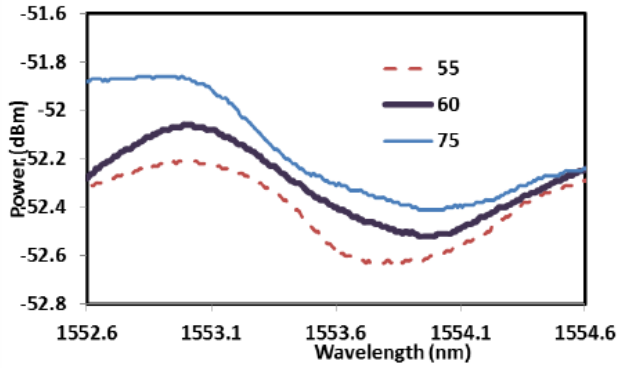

Fig. 7. The reflected interference spectrum at various levels of humidity.

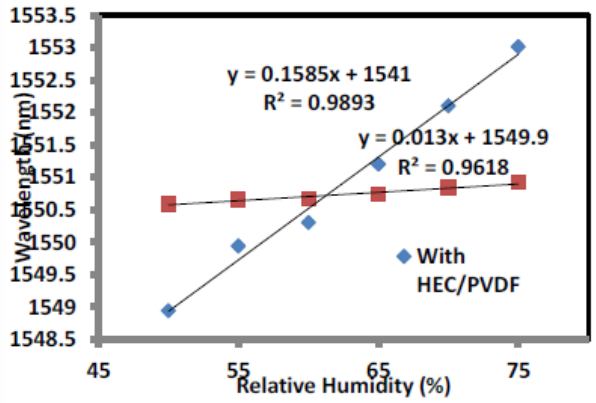

Fig. 8. The relationship between the interference peak wavelength against RH for the dumbbell MZI sensor with and without the HEC/PVDF coating.

3. Conclusion

A new dumbbell-shaped inline MZI is developed using an arcing process of a fusion splicer for sensing three physical parameters. The sensor probe consists of two bulges separated by a tapered waist that generates a good reflected interference spectrum where the FSR depends on the length of the waist. The interference spectrum shifts with the variations in the ambient temperature, refractive index and humidity. The experimental results show that the temperature sensitivity of the sensor is 0.049 nm/°C at the tapered waist length of 0.5 cm. The reflected interference spectrum is blue-shifted with the increase of the surrounding refractive index from 1.00 to 1.36. For relative humidity measurement, after the dumbbell MZI is coated with a HEC/PVDF composite, the reflected spectrum is linearly shifted to a longer wavelength when the relative humidity of the surrounding changes with a sensitivity of 0.159 nm/RH%. Its low fabrication cost, simple configuration and high sensitivity would attract many potential applications from various fields.

Acknowledgement

The authors acknowledge the financial support from the University of Malaya and Ministry of Higher Education (MOHE) under the High Impact Research Grant Scheme (Grant No: D000009-16001).

References

[1] C. L. Zhao, X. Yang, M. S. Demokan, W. Jin, Journal of lightwave technology, **24**(2), 879 (2006).
[2] X. Shu, B. A. Gwandu, Y. Liu, L. Zhang, I. Bennion, Optics Letters, **26**(11), 774 (2001).
[3] B. A. Gwandu, X. Shu, T. D. Allsop, W. Zhang, L. Zhang, D. J. Webb, I. Bennion, Electronics Letters, **38**(14), 695 (2002).
[4] Z. Tian, S. H. Yam, H. P. Loock, Photonics Technology Letters, IEEE, **20**(16), 1387 (2008).
[5] Y. Wang, M. Yang, D. N. Wang, S. Liu, P. Lu, JOSA B, **27**(3), 370 (2010).
[6] L. Jiang, L. Zhao, S. Wang, J. Yang, H. Xiao, Optics Express, **19**(18), 17591 (2011).
[7] T. Zhu, D. Wu, M. Deng, D. Duan, Y. Rao, X. Bao, 21st International Conference on Optical Fibre Sensors (OFS21) (pp. 77532P-77532P). International Society for Optics and Photonics (2011).
[8] J. Villatoro, D. Monzón-Hernández, D. Talavera, Electronics letters, **40**(2), 106 (2004).
[9] K. Q. Kieu, M. Mansuripur, Photonics Technology Letters, IEEE, **18**(21), 2239 (2006).
[10] D. Wu, T. Zhu, M. Deng, D. W. Duan, L. L. Shi, J. Yao, Y. J. Rao, Applied Optics, **50**(11), 1548 (2011).
[11] H. J. Patrick, A. D. Kersey, F. Bucholtz, Journal of Lightwave Technology, **16**(9), 1606 (1998).
[12] K. S. Chiang, Y. Liu, M. N. Ng, X. Dong, Electronics Letters, **36**(11), 966 (2000).
[13] Q. Wu, Y. Semenova, P. Wang, G. Farrell, Optics Express, **19**(9), 7937 (2011).
[14] G. A. Cárdenas-Sevilla, F. C. Fávero, J. Villatoro, Sensors, **13**(2), 2349 (2013).
[15] D. Wu, T. Zhu, K. S. Chiang, M. Deng, Journal of Lightwave Technology, **30**(5), 805 (2012).
[16] R. Yang, Y. S. Yu, Y. Xue, C. Chen, Q. D. Chen, H. B. Sun, Optics letters, **36**(23), 4482 (2011).
[17] A. A. Jasim, S. W. Harun, H. Arof, H. Ahmad, (2013).

*Corresponding author: ahamzah@um.edu.my